BMC Microbiology

RESEARCH Open Access

Whole-genome analysis of *Bacillus paranthracis* YC06 isolated from healthy individual feces for biodegrading inosine and guanosine

Xiaoyu Cao[1], Yu Zhang[1], Qianqian Xu[1] and Hai Yan[1*]

Abstract

The overproduction of uric acid, driven by its key precursors (inosine and guanosine), leads to hyperuricemia, a metabolic disorder associated with severe complications such as gout and renal dysfunction. Here, a promising bacterial strain YC06 with excellent biodegradation capability for inosine and guanosine was successfully isolated from healthy individual feces and identified as *Bacillus paranthracis* through average nucleotide identity (ANI) analysis. *B. paranthracis* YC06 resting cells (live but suspended in PBS buffer) and its cell-free extracts could effectively biodegrade inosine and guanosine in vitro. Whole-genome sequencing revealed a 5,535,183 bp draft genome (52 contigs, 35.22% GC content) containing 5,672 protein-coding genes. *B. paranthracis* YC06 demonstrated high survival rates in simulated gastrointestinal fluids, supported by the presence of stress-response genes and bile salt hydrolase genes associated with gastrointestinal tolerance. However, this strain exhibited hemolytic activity and no amino acid decarboxylase activity, while hemolysin genes, antibiotic genes and toxin-producing genes were identified, raising potential biosafety concerns for its further application. The gene functional annotation and polymerase chain reaction (PCR) amplification electrophoresis identified key genes (*rihA*, *rihB*, *deoD* and *pnp*) encoding purine nucleosidase and purine-nucleoside phosphorylase, and combined with biodegradation product analysis, elucidated the pathways of inosine and guanosine biodegradation into hypoxanthine and guanine. Comprehensive safety evaluations, including cytotoxicity assay and in vivo pathogenicity studies, must be conducted to rigorously assess its risks prior to practical utilization.

Keywords *Bacillus paranthracis* YC06, Whole-genome analysis, Inosine, Guanosine, Biodegradation

*Correspondence:
Hai Yan
haiyan@ustb.edu.cn
[1]School of Chemistry and Biological Engineering, University of Science and Technology Beijing, Beijing 100083, China

Introduction

Hyperuricemia, a metabolic disorder arising from the overproduction and/or underexcretion of uric acid (the final product of purine metabolism in humans), is defined by serum uric acid levels exceeding 6.8 mg/dl and is associated with an elevated risk of gout [1, 2], cardiovascular disease [3], chronic kidney disease [4] and metabolic syndrome [5] risk. Recent statistics reveal that the prevalence of hyperuricemia in mainland China has increased noticeably, 22.7% among men and 11.0% among women [6], compared to 20.2% in men and 20.0% in women in U.S [7]. Up to now, the management of hyperuricemia could be divided into two approaches: pharmacological and nonpharmacological therapy [8, 9]. Hyperuricemia is commonly treated with chemical drugs such as allopurinol, febuxostat, and benzbromarone, but long-term use of chemical drugs can cause hepatorenal dysfunction and allergic reactions [10]. However, nonpharmacological approaches, including diet modification and regular exercise, are also recommended but often prove less effective due to challenges in sustained patient compliance [9]. According to the current situation, more efficient and secure management methods of hyperuricemia need to be developed.

Inosine and guanosine are significant uric acid precursors, which could be converted to hypoxanthine and guanine by purine-nucleoside phosphorylase (PNP) or purine nucleosidase, respectively [11, 12]. Emerging research indicates that the degradation of intestinal nucleosides into nucleobases impairs their absorption capacity by small intestinal epithelial cells [7]. This metabolic shift consequently reduces dietary purine intake, thereby contributing to decreased endogenous uric acid production [13].

In recently years, many bacterial strains isolated from diverse fermented foods have shown the inosine and guanosine degradation ability, including *Lacticaseibacillus rhamnosus* Fmb14 isolated from traditional fermented Chinese yogurt [14], *Lactiplantibacillus plantarum* isolated from Chinese sauerkraut [15], *Lactobacillus acidophilus* F02 isolated from traditional fermented sourdough [16], and *Lactobacillus fermentum* 9 – 4 isolated from Chinese fermented rice-flour noodles [17]. However, the relationship between gut microbiota and hyperuricemia has been extensively studied, and gut microbiota has gradually emerged as a novel therapeutic target for hyperuricemia management [18]. Most of uric acid is excreted through the kidneys, but more and more researches have shown that intestinal tract plays a key role in uric acid excretion, as around 1/3 of uric acid is excreted through intestine [19, 20]. Notably, comparative analyses have demonstrated significant divergence between the gut microbiomes of hyperuricemia patients and healthy controls [21].

The objective of this study is to isolate and identify microbial strains from the gut microbiota of healthy individuals that possess the capability to biodegrade inosine and guanosine. We have successfully isolated a novel *Bacillus paranthracis* strain using inosine and guanosine as the sole carbon and nitrogen source, designated YC06. *Bacillus* species demonstrate superior advantages as probiotics compared to lactic acid bacteria, owing to their inherent high tolerance to harsh environmental conditions [22]. Currently commercialized *Bacillus* probiotics include *B. subtilis*, *B. cereus*, and *B. coagulans*, among others. Through comprehensive whole-genome analysis coupled with subsequent polymerase chain reaction (PCR) product validation, the key enzymatic genes involved in the biodegradation of inosine and guanosine were identified. Furthermore, the potential probiotic properties and safety profile of *B. paranthracis* YC06 at the gene level were also explored by whole-genome analysis, and it was preliminarily confirmed by in vitro assays.

Materials and methods

Chemicals and samples

Above 99% purity of inosine, guanosine, hypoxanthine and guanine were obtained from Shanghai Aladdin Biochemical Technology Co., Ltd (Shanghai, China). Bile salt (cholic acid content > 75.0%), Pepsin (3000 U/mg) and Trypsin (Biotech) were purchased from Macklin Biochemical Co., Ltd (Shanghai, China). All other chemicals used for experiments were analytical or chromatographic reagent. Strain YC06 was isolated from the healthy individual feces, which obtained from Beijing Fumate Biotechnology Co., Ltd. (Beijing, China).

Isolation of the bacterial strain with inosine and guanosine biodegrading ability

From the feces samples, strain YC06 was isolated in the medium (0.1 g inosine, 0.1 g guanosine, 0.05 g $Na_2HPO_4 \cdot 2H_2O$, 0.05 g $KH_2PO_4 \cdot 3H_2O$, 0.01 g $MgSO_4$, 0.001 g $CaCl_2$, 0.1 mL trace element solution and 1.8 g agar, per 100 mL, initial pH 7.0). Strain YC06 was subsequently transferred to a liquid medium with both inosine and guanosine as the sole carbon and nitrogen source and incubated at 37 ℃ for 24 h. After serial dilution and streaking on LB agar plates, a single colony of strain YC06 was isolated, activated in LB medium, and preserved in 50% glycerol at -20 ℃. *Staphylococcus aureus* CICC 21,600 and *Escherichia coli* CICC 10,664 were cultured in LB medium under the same conditions as above.

LB medium contained (g/L): NaCl, 10; Peptones, 10; Glucose, 5; Yeast powder, 5 and H_2O 1 L. All mediums were sterilized in an autoclave (LDZH-100 L, Shanghai, China) at 121 ℃ for 20 min.

Determination biodegradation ability of inosine and guanosine by *B. paranthracis* YC06

To evaluate the biodegradation ability of inosine and guanosine, strain YC06 was inoculated to LB medium and cultured at 37 ℃ for 18 h (late log phase). 2 mL of *B. paranthracis* YC06 culture solution was centrifuged (Pingke PK-16 A, Changsha, China) at 4 ℃, 8,000 ×g for 15 min, and then the harvested cells were washed twice with 1 mL phosphate buffer solution (PBS, 0.1 M, pH 7.4), resuspended in 750 µL of inosine or guanosine solution [15]. Another culture solution was treated with the same pretreatment, after which the cell lysis was performed for 25 min with an output power of 360 W by an ultrasonic homogenizer (JY92-IIDN, SCIENTZ, Ningbo, China). The supernatant as cell-free extracts (CEs) was obtained by centrifugation at 6,000 ×g for 15 min at 4 ℃, and the protein concentration was determined using BCA protein assay kit (Beyotime, Shanghai, China) [23].

Subsequent biodegradation experiments by YC06's resting cells (10^7 CFU/mL) and CEs should be elaborated at 37 ℃ for 12 h (no shaking, initial concentration of inosine or guanosine: 1 g/L). And samples were taken at different times for determining inosine and guanosine concentration by high performance liquid chromatography (HPLC, Shimadzu LC-20AT, Tokyo, Japan).

Whole genome sequencing and genome annotation

Genomic DNA of YC06 was extracted using MagPure Bacterial DNA Kit (D6361-02, Magen, Shanghai, China). DNA concentration was determined via Qubit4.0 (Thermo, Q33226). DNA integrity was assessed by 1% agarose gel electrophoresis. The whole genome DNA was randomly fragmented to an average size of 200–400 bp. The selected fragments were through end-repair, 3' adenylated, adapters-ligation, PCR amplifying. After purification with the magnetic beads, the library was qualified by the Qubit 4.0 fluorometer and the length of library was assessed by the 2% agarose gel electrophoresis. The qualified libraries were sequenced on the MGI DNBSEQ-T7 platform at Sangon Biotech (Shanghai, china).

After sequencing, raw reads were filtered via Trimmomatic (v0.36) by removing adaptors and low-quality reads, then clean reads were obtained. Genome assembly was done using SPAdes (v3.15) and the Gapfiller (v1.11) was used for filling gaps. The Whole Genome Shotgun project has been deposited at NCBI under the accession JBNFTL000000000.

Gene predictions and annotations were generated using the the Prokka (Version 1.10) and NCBI NR database. The functional annotation of genes was mainly based on protein coding genes using the Cluster of Orthologous Groups of proteins (COG, https://www.ncbi.nlm.nih.gov/COG/), Gene Ontology (GO, http://www.geeontology.org), and the Kyoto Encyclopedia of Genes and Genomes (KEGG, http://www.kegg.jp). The Virulence Factor Database (http://www.mgc.ac.cn/VFs/main.htm) and Comprehensive Antibiotic Resistance Database (https://card.mcmaster.ca/) were queried to predict the virulence genes and antibiotic resistance genes.

Identification of strain YC06

Phylogenetic analysis was conducted based on 16 S rDNA and average nucleotide identity (ANI) compared against genomic sequences. For the ANI analysis, the chromosomal sequences of eight strains were downloaded from the GenBank database. The ANI values were calculated using OrthoANI tool (https://www.ezbiocloud.net/tools/orthoani), and then a heatmap was generated to visually represent the genetic similarities among the strains based on the results.

Tolerance of *B. paranthracis* YC06 in simulated gastrointestinal fluids

The tolerance of *Bacillus* genus to simulated gastrointestinal fluids were determined according to the previous report with modifications [24]. Simulated gastric environment juice: 7.3 g/L NaCl, 0.5 g/L KCl, 3.8 g/L $NaHCO_3$, 3.0 g/L Pepsin, adjust pH 2.5 using 1 M HCl. Simulated intestinal environment juice: 2.6 g/L NaCl, 1.0 g/L Trypsin, 3.0 g/L Bile salt, adjust pH 8.0 using 0.5 M NaOH [25].

B. paranthracis YC06 was inoculated into LB medium and cultured at 37 ℃ for 24 h. The obtained strain YC06 cultures were centrifuged at 4 ℃, 8,000 ×g for 15 min, and then the precipitated cells were washed twice and resuspended using stroke-physiological saline solution. 100 µL of suspension was added into 900 µL simulated gastric (performed for 90 min) and intestinal juice (performed for 180 min), respectively. In the control group, 100 µL of the suspension was mixed with 900 µL of stroke-physiological saline solution. Furthermore, comparative tolerance assays were performed using *Lacticaseibacillus casei* CICC 6114, a well-characterized probiotic strain, to benchmark the physiological robustness of our experimental findings. Finally, the samples were diluted and streaked on the LB plate for viable bacteria count, and 3 parallel samples were made for each sample.

The survival rate was calculated according to the following formula: (St/Sc) ×100%, where St: Viable count after simulated gastric or intestinal juice treatment (CFU/mL), Sc: Viable count after stroke-physiological saline solution treatment at same time (CFU/mL).

Hemolytic activity

Hemolytic assay of *B. paranthracis* YC06 was carried out using Columbia blood agar (Babio, Qingdao, China) as

described by previous research [26]. *S. aureus* was used as positive control for hemolytic activity.

Amino acid decarboxylase test

Refer to previous study methods [27], *B. paranthracis* YC06 cell suspension (100 µL) were inoculated into micro-biochemical identification tube containing different amino acids (lysine, ornithine, and arginine) (Hopebio, Qingdao, China) and amino acid decarboxylase control, respectively. Then 300 µL of sterilized liquid paraffin was added into each tube and incubated at 37 ℃ for 24 h. The color changes in the broth were observed, and *E. coli* was used as positive control.

Analysis of inosine and guanosine and biodegradation products by HPLC

The samples were diluted 10 times using 0.5 M NaOH solution and centrifuged at 8,000 ×g for 15 min. The supernatant was used to detect concentration levels, which passed through an aqueous phase microporous membrane (0.22 µm). The separation condition for HPLC were as follows: Kromasil C18 (4.6 × 250 mm, 5 µm-Micron); UV detection wavelengths of 253 nm and 248 nm; the mobile phase was methanol: 0.5% acetic acid aqueous solution (10:90); the injection volume was 20 µL; with a flow rate of 1 mL/min and column temperature of 35 ℃. The standard curve between the content (20, 40, 60, 80, 100 mg) and peak area of inosine, guanosine, hypoxanthine and guanine were established, and all of the correlation coefficient of standard curves regression equation were $R^2 > 0.999$. All experiments were conducted in triplicates and were subjected to statistical analysis.

PCR

The genomic DNA of strain YC06 was used as a template to amplify genes *rihA*, *rihB*, *deoD*, *punA* and *pnp*. Primers used are available in Table S1.

Results

Isolation and identification of strain YC06

The monoclonal colonies of *B. paranthracis* YC06 were off-white, circular, non-translucent and 3–5 mm in diameter after incubation at 37 ℃ for 24 h on LB agar plate (Fig. 1a). The central elliptical endospore was observed under a light microscope with 1000× magnification (Fig. 1b). 16 S rDNA sequencing analysis confirmed that strain YC06 belongs to the genus *Bacillus*. The genome of YC06 was 98.52% identical by ANI to the genome of *B. paranthracis* Gxun-30 (Fig. 1c).

Biodegradation of inosine and guanosine by YC06's resting cells and its CEs

To determinate the inosine and guanosine biodegrading ability of *B. paranthracis* YC06, its cells were added to the PBS solution containing inosine or guanosine for cultivation. Results showed that YC06's resting cells could effectively biodegrade inosine and guanosine within 8 h (Fig. 2a), and the biodegradation ratio for inosine is better than that of guanosine. Meanwhile, its CEs, which contain a protein concentration of 0.37 g/L, could remove 0.46 g/L of guanosine and 0.68 g/L of inosine within 9 h (Fig. 2b). The HPLC results depicted the presence of characteristic peaks corresponding to both inosine and guanosine, along with their metabolic products, throughout the biodegradation process (Fig. S1). Alternatively, HPLC results revealed absorption peaks of biodegradation products of inosine and guanosine at 4.46 and 4.38 respectively, which was consistent with the standard of hypoxanthine and guanine peaks.

Overview of genome analysis

The whole-genome sequencing analysis and gene functions annotation were performed in *B. paranthracis* YC06. The total number of bases after quality control was 1,367,713,016 bp. The integrity of the initial genome sequence assemblies was evaluated, and the outcomes indicated a high-quality assembly, which is suitable for subsequent detailed analyses (Fig. S2). The whole-genome sequence of strain YC06 was 5,535,183 bp with an average GC content of 35.80%. The reads were assembled into 52 contigs with an N50 of 341,019 bp. The total length of the predicted protein-coding genes (CDS) was 4,675,722 bp, and genome predicted 96 tRNA genes, 10 rRNA genes and 1 ncRNA genes. All the detailed parameters are shown in Table S2. *B. paranthracis* YC06 had similar genomic GC content and genome size compared with other reported *Bacillus paranthracis* strains [26].

The 3,266 protein-coding genes of *B. paranthracis* YC06 were functionally classified using the COG database, revealing 21 distinct functional categories (Fig. 3a). Notably, 122 genes were associated with nucleotide transport and metabolism. GO annotation categorized 835 genes into three ontological groups: biological processes, molecular functions, and cellular components (Fig. 3b). KEGG pathway analysis assigned 1,333 genes to five major functional categories, with 110 genes specifically involved in nucleotide metabolism pathways (Fig. 3c). In addition, 5660 protein-coding genes of *B. paranthracis* YC06 were annotated using the NR database, 2043 genes using CDD, and 3493 genes using Pfam (Fig. S3).

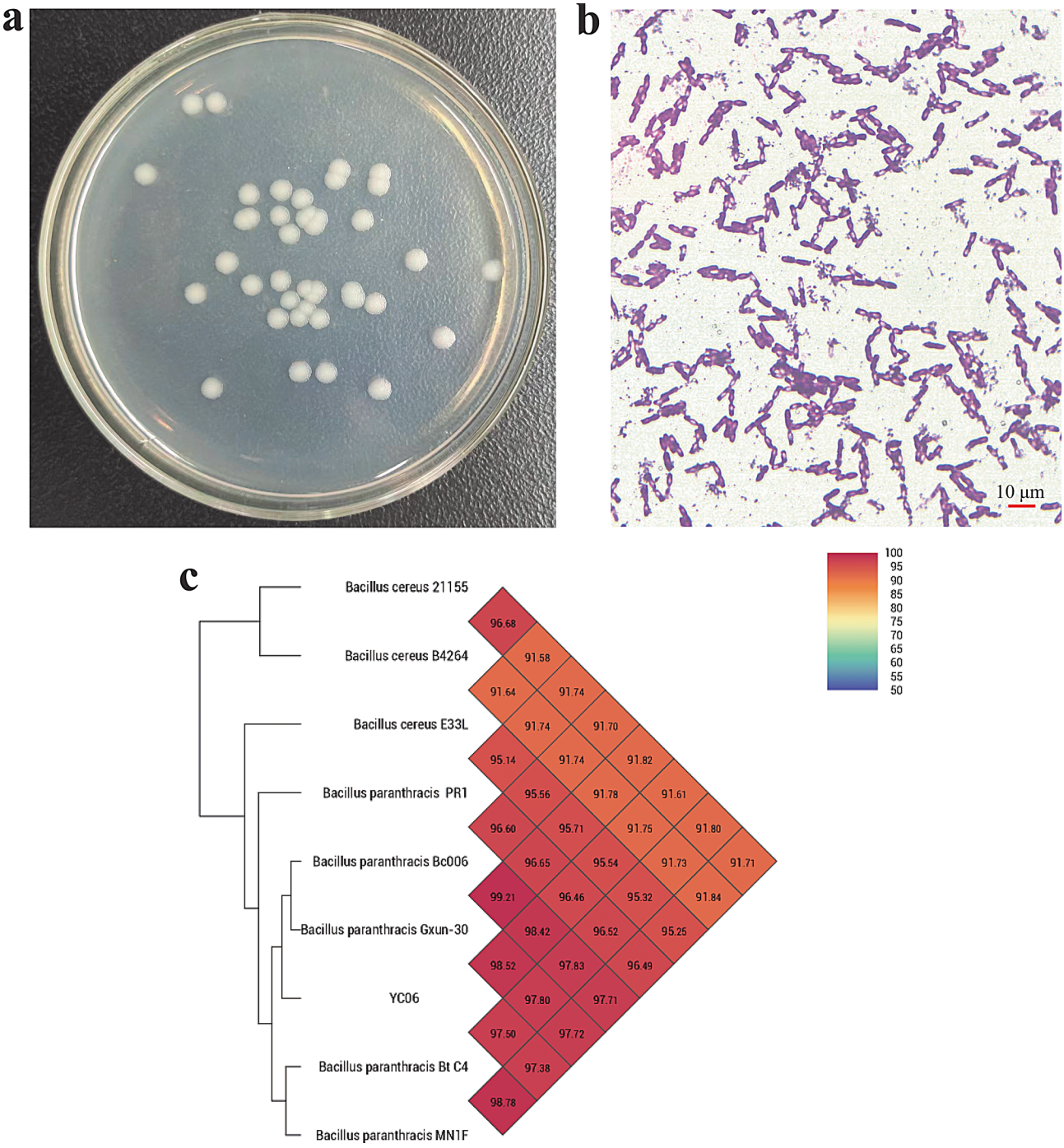

Fig. 1 Isolating inosine and guanosine biodegrading strain YC06. Colonies were grown on LB agar plate (**a**); morphology (1000×) under the microscope (**b**); and heat map of average nucleotide identity (c)

Comparative and pan-genome analysis of 8 *B. paranthracis* strains

A comparative genomic and pan-genome analysis was conducted to assess the diversity of genes within *B. paranthracis* strains (Table S3). This involved a comparison with the genomes of 8 *B. paranthracis* strains (Fig. 4a). All the eight *B. paranthracis* strains shared 3645 genes. Genes that are found only in each strain from *B. paranthracis* Gxun-30, NCCP 15,910, YC06, Bc006, Bt C4, SSBC101, KF11, SHOU-BC01 are 96, 248, 842, 349, 156, 202, 79 and 130, respectively. Most of the specific genes are hypothetical proteins. Pangenome analysis of the *B. paranthracis* pan-genome revealed the presence of

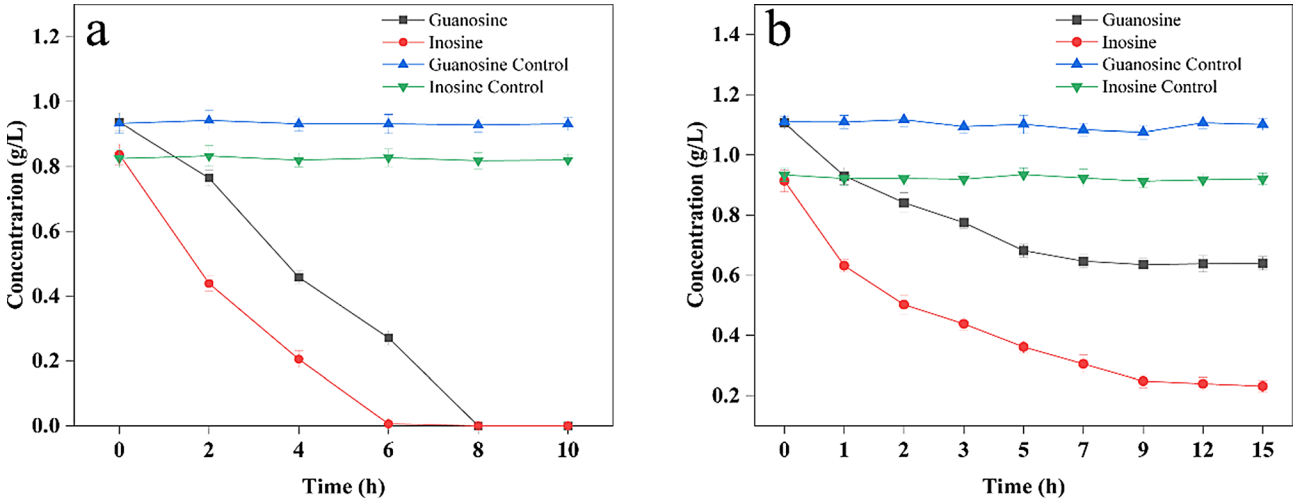

Fig. 2 Biodegradation of inosine and guanosine by *B. paranthracis* YC06's resting cells (**a**) and its CEs (**b**). Data are expressed as mean ± SD from three independent biological replicates ($n = 3$)

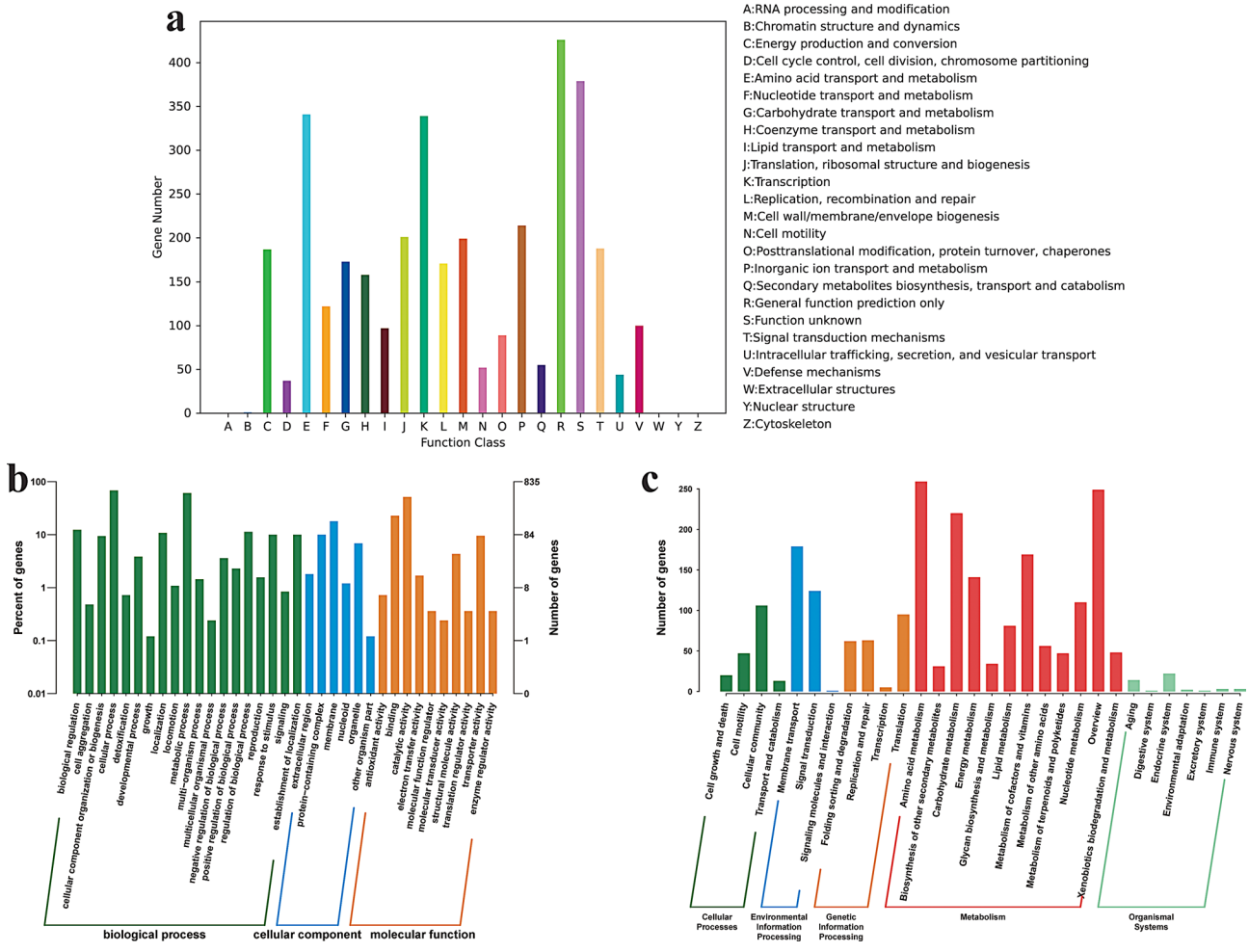

Fig. 3 Statistical legend of gene annotation classification of *B. paranthracis* YC06. COG function classification (**a**), GO function classification (**b**), Histogram of KEGG (**c**)

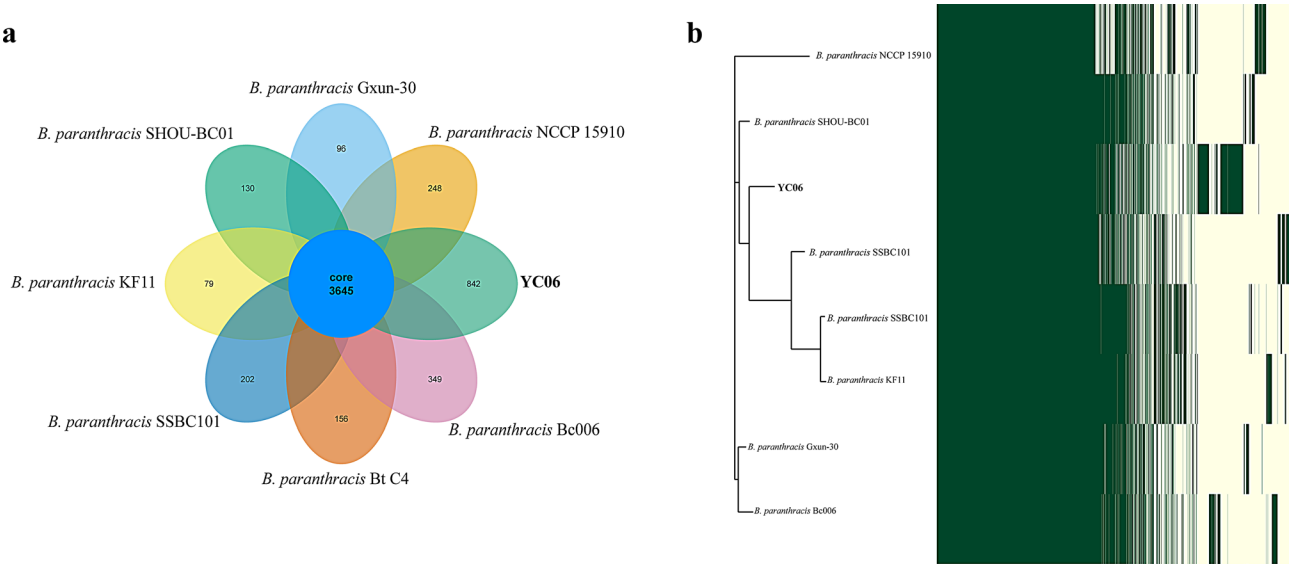

Fig. 4 Comparative analysis of genes annotated among 8 *B. paranthracis* strains. Venn diagram showed different number of unique and sharing genes among the *B. paranthracis* genome (**a**). Pan-genome presented a core and accessory gene by comparing with the genomes of *B. paranthracis* (**b**)

3645 core genes, along with 2348 dispensable genes and 2102 specific genes (Fig. 4b).

Genetic features and in vitro probiotic assays of *B. paranthracis* YC06

Survivability in the gastrointestinal tract is a crucial measure of probiotics' beneficial functions within the human body [28]. Upon passing through the stomach, probiotics reach the duodenum where they are subjected to various stress conditions, notably the presence of bile salts [29]. As a potential probiotic, strain YC06 must maintain survival in harsh conditions, which remains active after passing through gastrointestinal environment (low pH, bile and protease). Strain YC06 demonstrated exceptional gastrointestinal tolerance, retaining 76.3 ± 2.1% viability after 90 min exposure to simulated gastric fluid (pH 2.5) and 53.8 ± 1.9% survival in 0.3% bile salt-containing intestinal fluid (pH 8.0), outperforming the probiotic benchmark strain *Lacticaseibacillus casei* CICC 6114, which showed a 1–2 order of magnitude reduction in survival under equivalent treatment conditions.

Whole-genome analysis revealed that multiple genes play a key role in survival in harsh conditions (Table 1). To assess acid resistance mechanisms, we screened the genome of *B. paranthracis*. YC06 for homologs of the glutamate-dependent acid resistance (GDAR) system characterized in *E. coli* [30]. The *atp* gene is essential in maintaining neutral pH in the bacterial cytosol [31]. Besides, *B. paranthracis* YC06 genome analysis also revealed *mdh* gene that encode for lactate synthesis, which associated with antimicrobial activity and acid tolerance [32]. Bile salts serve multiple functions, including the dispersion and absorption of lipids, and also possess surfactant properties that can disrupt the integrity of the cell membrane [33]. They are capable of producing free radicals and altering intracellular pH levels. Bile salts can undergo deconjugation through the action of bile salt hydrolase (*bsh*) and are subsequently reabsorbed in the colon [34]. These results underscore the robustness of *B. paranthracis* YC06 in the face of the challenging conditions encountered in the gastrointestinal tract, which is a promising attribute for its potential application as a probiotic.

Safety properties

In YC06 genome, total of 397 putative virulence factor genes were found. Among these virulence factors, only eight genes exhibited a similarity exceeding 70%, which indicated high similarity to the genes in VFDB database (Table 2). Genomic annotation of *B. paranthracis*YC06 revealed the presence of virulence-associated genes *cytK*, *nheA*, and *nheB*, which encode putative cytotoxin K and non-hemolytic enterotoxin components, respectively. These genes are implicated in hemolytic and cytotoxic activities [35]. Consistent with this genomic profile, in vitro hemolytic assay demonstrated that strain YC06 exhibited β-hemolytic activity, forming distinct zones of clearance on Columbia blood agar plates after 24 h of incubation at 37 ℃ (Fig. S4a). Furthermore, genomic analysis identified the absence of genes encoding amino acid decarboxylases (e.g., *hdc*, *ldc*, or *odc*), which are typically associated with biogenic amine production [36]. This genomic finding was corroborated by phenotypic assays, as the activity of amino decarboxylase in *B. paranthracis* YC06 is negative (Fig. S4b). Compared to ARDB database, five putative antibiotic resistance genes

Table 1 Potential genes related to different probiotic properties from *B. paranthracis* YC06 genome

Gene ID	Location	Start	End	Length (bp)	Gene name	Product	Function
gene4339	Contig11	134,353	138,789	4437	*gltB*	Glutamate synthase [NADPH] large chain	Acid stress
gene4103	Contig10	57,618	58,001	384	*gcvH*	Glycine cleavage system H protein	Acid stress
gene3997	Contig9	120,951	122,051	1101	*gcvT*	minomethyltransferase	Acid stress
gene3996	Contig9	119,587	120,930	1344	*gcvP*	putative glycine dehydrogenase (decarboxylating) subunit	Acid stress
gene2763	Contig5	113,918	114,442	525	*speG*	Spermidine N (1)-acetyltransferase	Acid stress
gene2762	Contig5	112,676	113,875	1200	*metK*	S-adenosylmethionine synthase	Acid stress
gene649	Contig1	621,110	621,463	354	*yjbR*	putative protein YjbR	Acid stress
gene3508	Contig7	167,642	169,150	1509	*atpA*	ATP synthase subunit alpha	Acid stress
gene3506	Contig7	164,881	166,287	1407	*atpD*	ATP synthase subunit beta	Acid stress
gene3505	Contig7	164,459	164,860	402	*atpC*	ATP synthase epsilon chain	Acid stress
gene3507	Contig7	166,529	167,389	861	*atpG*	ATP synthase gamma chain	Acid stress
gene3509	Contig7	169,162	169,704	543	*atpH*	ATP synthase subunit delta	Acid stress
gene3512	Contig7	170,612	171,331	720	*atpB*	ATP synthase subunit a	Acid stress
gene3510	Contig7	169,701	170,207	507	*atpF*	ATP synthase subunit b	Acid stress
gene3511	Contig7	170,337	170,555	219	*atpE*	ATP synthase subunit c	Acid stress
gene3779	Contig8	168,344	169,375	1032	*recA*	Protein RecA	Acid stress
gene3283	Contig6	254,775	255,386	612	*sodA*	Superoxide dismutase [Mn]	Acid stress
gene345	Contig1	346,044	347,003	960	*relA*	GTP pyrophosphokinase	Acid stress
gene2328	Contig4	198,066	199,505	1440	*aspA*	Aspartate ammonia-lyase	Acid stress
gene3159	Contig6	140,012	141,787	1776	*aspS*	Aspartate-tRNA ligase	Acid stress
gene383	Contig1	384,385	385,122	738	*gpmA*	2,3-bisphosphoglycerate-dependent phosphoglycerate mutase	Acid stress/ Bile tolerance
gene5539	Contig23	17,147	18,526	1380	*glmU*	Bifunctional protein GlmU	Acid stress/ Bile tolerance
gene2733	Contig5	87,705	88,178	474	*luxS*	S-ribosylhomocysteine lyase	Bile tolerance
gene2547	Contig4	402,940	404,085	1146	*bshA*	N-acetyl-alpha-D-glucosaminyl L-malate synthase	Bile tolerance
gene2548	Contig4	404,082	404,786	705	*bshB*	N-acetyl-alpha-D-glucosaminyl L-malate deacetylase	Bile tolerance
gene3636	Contig8	16,776	18,392	1617	*bshC*	Putative cysteine ligase BshC	Bile tolerance
gene5601	Contig24	24,730	25,518	789	*nagB*	Glucosamine-6-phosphate deaminase	Bile tolerance
gene3539	Contig7	193,303	194,910	1608	*pyrG*	CTP synthase	Bile tolerance
gene103	Contig1	104,274	105,962	1689	*argS*	Arginine–tRNA ligase	Bile tolerance
gene2898	Contig5	232,980	233,582	603	*rpsD*	30 S ribosomal protein S4	Bile tolerance
gene5481	Contig22	37,342	38,001	660	*rpsC*	30 S ribosomal protein S3	Bile tolerance
gene5492	Contig22	41,874	42,374	501	*rpsE*	30 S ribosomal protein S5	Bile tolerance
gene5461	Contig22	17,870	18,295	426	*rplK*	50 S ribosomal protein	Bile tolerance
gene5476	Contig22	34,868	35,491	624	*rplD*	50 S ribosomal protein L4	Bile tolerance
gene5487	Contig22	39,700	40,239	540	*rplE*	50 S ribosomal protein L5	Bile tolerance
gene5490	Contig22	40,919	41,458	540	*rplF*	50 S ribosomal protein L6	Bile tolerance
gene319	Contig1	321,222	321,425	204	*cspA*	Major cold shock protein CspA	Temperature stress
gene1076	Contig2	160,048	160,248	201	*cspD*	Cold shock-like protein CspD	Temperature stress
gene3246	Contig6	219,697	221,532	1836	*dnaK*	Chaperone protein DnaK	Temperature stress
gene3247	Contig6	221,737	222,852	1116	*dnaJ*	Chaperone protein DnaJ	Temperature stress
gene4559	Contig13	28,056	30,053	1998	*katE*	Catalase HPII	Oxidative stress
gene45	Contig1	40,982	41,464	483	*gpx*	Hydroperoxy fatty acid reductase gpx	Oxidative stress
gene2914	Contig5	249,544	250,044	501	*tpx*	Thiol peroxidase	Oxidative stress
gene1458	Contig2	512,612	512,917	306	*arsR*	Arsenical resistance operon repressor	Oxidative stress
gene1461	Contig2	514,501	514,905	405	*arsC*	Arsenate reductase	Oxidative stress
gene3421	Contig7	78,141	79,499	1359	*arsB*	Arsenical pump membrane protein	Oxidative stress
gene3039	Contig6	22,487	22,801	315	*trxA*	Thioredoxin	Oxidative stress
gene2589	Contig4	437,634	438,614	981	*trxB*	Thioredoxin reductase	Oxidative stress
gene2964	Contig5	294,161	295,099	939	*mdh*	Malate dehydrogenase	Lactate synthesis

Table 2 Putative virulence factors in *B. parathracis* YC06 genome

Gene ID	Location	Gene name	Predicted functions	Identify (%)
gene1929	Contig3	*cytK*	Haemolytic and cytotoxic activity	99.4
gene2249	Contig4	*nheB*	Pore-forming toxin	98.8
gene5321	Contig20	*inhA*	A secreted and cell associated protease; a regulatory factor of adhesin BslA expression	98.4
gene2250	Contig4	*nheA*	Pore-forming toxin	97.4
gene1310	Contig2	*BAS*3109	Lytic activity against phagocytes and decreases the barrier function of human polarized epithelial cells	94.9
gene3191	Contig6	*lap*	Promotes bacterial adhesion to intestinal cells	73.9
gene3342	Contig6	*clpP*	Serine protease involved in proteolysis and is required for growth under stress conditions	70.7
gene5869	Contig7	*clpP*		

Table 3 Putative antibiotic resistance genes in *B. parathracis* YC06 genome

Gene ID	Location	Gene name	Antibiotics	Gene family	Identify (%)
gene1159	Contig2	*BcII*	cephalosporin; penam	subclass B1 *Bacillus cereus* Bc beta-lactamase	98.4
gene395	Contig1	*Bla1*	penam	class A *Bacillus anthracis* Bla beta-lactamase	94.4
gene495	Contig1	*tet(45)*	tetracycline	major facilitator superfamily (MFS) antibiotic efflux pump	88.6
gene2672	Contig10	*vanR*	glycopeptide	glycopeptide resistance gene cluster; vanR	77.6
gene1510	Contig7	*rphB*	rifamycin	rifampin phosphotransferase	72.3

associated with cephalosporin (*BcII*), β-lactam antibiotic (*Bla1*), tetracyclines (*tet(45)*), glycopeptide (*vanR*) and rifamycin (*rphB*) were annotated (Table 3).

Inosine and guanosine metabolic pathways

Given that purine metabolism is a complex process involving multiple factors, we further analyzed the associated pathways in the KEGG database (Fig. 5a). Whole-genome analysis of *B. paranthracis* YC06 identified two key enzymes (EC 2.4.2.1 and EC 3.2.2.1) implicated in the catabolism of inosine and guanosine (Fig. 5a). The genomic annotation of these enzymes (Table 4) was experimentally validated through PCR amplification (Fig. 5b). In vitro assays demonstrated that these intermediates of purine metabolism are biodegraded by purine nucleosidase or purine nucleoside phosphorylase (PNP) to form hypoxanthine and guanine [17]. Specifically, EC 2.4.2.1 (purine-nucleoside phosphorylase) catalyzes the phosphorolysis of nucleosides into sugars and nitrogenous bases, while EC 3.2.2.1 (purine nucleosidase) removes amino groups from nucleosides to generate analogs. The presence of these enzymatic activities suggests that *B. paranthracis* YC06 possesses a functional pathway for purine nucleoside degradation, which may contribute to hyperuricemia and gout pathogenesis [37].

Discussion

In this study, *B. paranthracis* YC06 with the biodegradation capability toward inosine and guanosine, was isolated from healthy individual feces sample. *B. paranthracis* is a novel species of the *B. cereus* group [38]. *Bacillus* species are an integral part of the normal gut microbiota [39], making the gastrointestinal tract a significant reservoir for probiotic *Bacillus* strains. These *Bacillus* strains have co-evolved with their hosts over a long period, thereby adapting well to the host's intestinal environment, facilitating their colonization and growth within the gut. Harnessing this understanding, the development of live biotherapeutic product (LBP) derived from these indigenous *Bacillus* strains could offer enhanced specificity and targeted therapeutic effects.

To the best knowledge of authors, HPLC results indicate that *B. paranthracis* YC06 has a better ability in the biodegradation of inosine and guanosine than any other bacterial reported. *B. paranthracis* YD01, which isolated from the healthy human intestine, could just biodegrade an initial concentration of 0.05 g/L of inosine or guanosine within 12 h [40]. In the gene functional annotation of *B. paranthracis* YD01, only purine nucleosidase (EC 3.2.2.1) was annotated as the enzyme responsible for metabolizing inosine and guanosine into hypoxanthine and guanine, respectively. Notably, no downstream degradation products were detected in their study, suggesting potential gaps in the metabolic pathway characterization. In the exploration of the degradation capabilities of different microbes towards inosine and guanosine, it has been observed that *Bacillus* exhibit a significantly higher efficiency in biodegradation compared to lactic acid bacteria. *Lacticaseibacillus rhamnosus* Fmb14, which live bacterial (10^7 CFU/mL) could degrade 0.13 g/L inosine within 3 h [14]. The live whole-cell and CEs of *Lactiplantibacillus plantarum* (10^7 CFU/mL) also degraded no

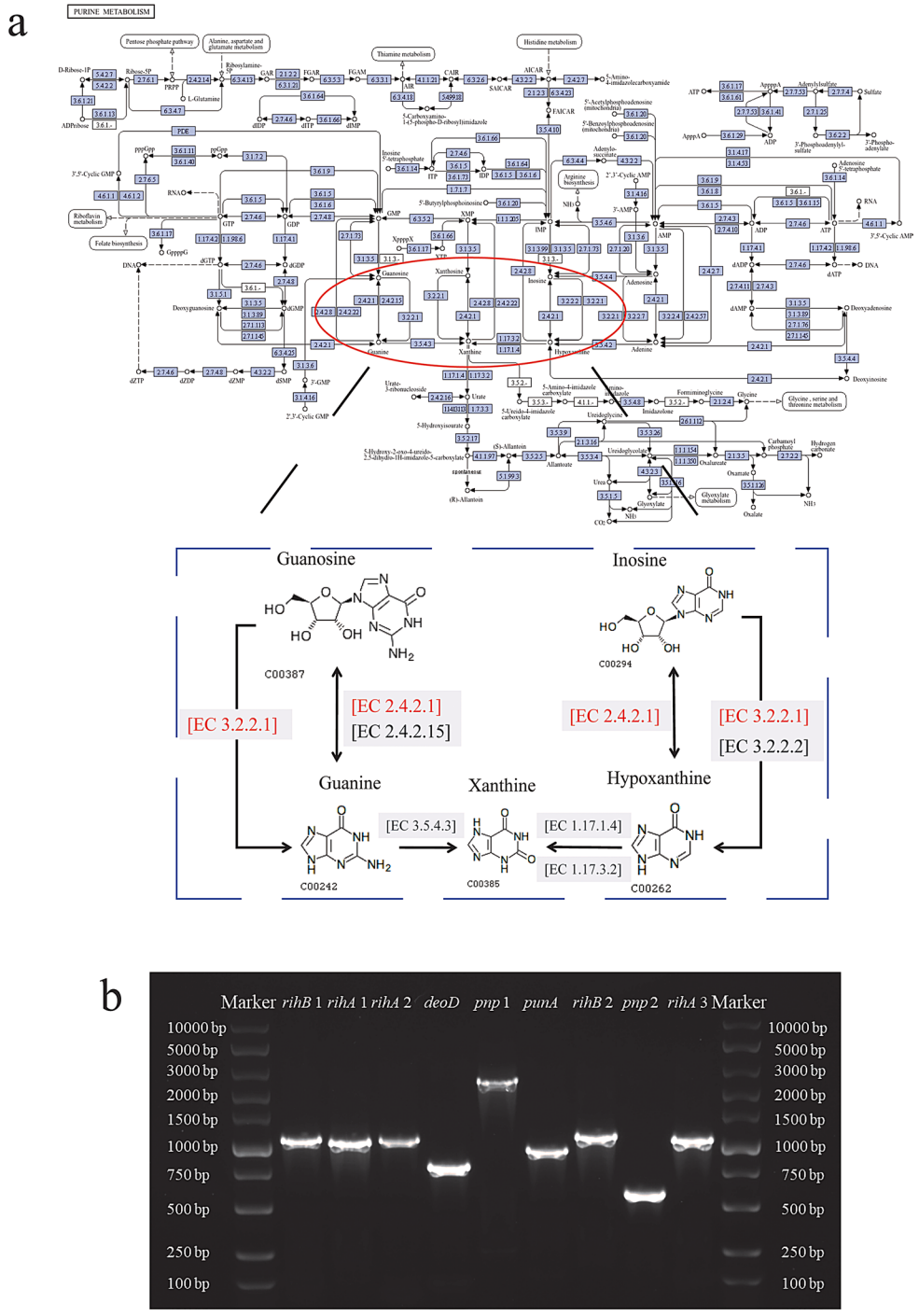

Fig. 5 The proposed metabolic pathway for biodegrading inosine and guanosine and corresponding functional genes of *B. paranthracis* YC06. Inosine and guanosine metabolic pathways (**a**). Amplification results of genes encoding enzymes (**b**)

more than 90% of inosine and guanosine at an initial concentration of 0.35 g/L and 0.37 g/L [15]. Living cells (10^9 CFU/mL) of *Lactobacillus acidophilus* F02 achieved 90% or 60% degradation rate of inosine or guanosine at an initial concentration of approximately 2.0 g/L [16].

The superior biodegradation capability of Bacilli may be attributed to their unique enzymatic systems and metabolic pathways, which enable them to handle purine nucleosides more efficiently. Moreover, the tolerance and adaptability of Bacilli allow them to maintain high biodegradation activity under variable environmental conditions, as confirmed in vitro simulated gastrointestinal environment experiments. Subsequent integration of HPLC results with whole-genome analysis has shed

Table 4 Genes and corresponding enzymes involved in inosine and Guanosine biodegradation

Gene ID	Location	Start	End	Length (bp)	Gene name	Enzyme	EC
gene0295	Contig1	303,230	304,169	939	*rihB* 1	purine nucleosidase	3.2.2.1
gene0746	Contig1	706,942	707,908	966	*rihA* 1	purine nucleosidase	3.2.2.1
gene1063	Contig2	143,133	144,066	933	*rihA* 2	purine nucleosidase	3.2.2.1
gene2621	Contig4	466,807	467,515	708	*deoD*	purine-nucleoside phosphorylase	2.4.2.1
gene3752	Contig8	138,392	140,531	2139	*pnp* 1	purine-nucleoside phosphorylase	2.4.2.1
gene3859	Contig9	2470	3292	822	*punA*	purine-nucleoside phosphorylase	2.4.2.1
gene5137	Contig18	5108	6059	951	*rihB* 2	purine nucleosidase	3.2.2.1
gene5551	Contig23	29,790	30,273	483	*pnp* 2	purine-nucleoside phosphorylase	2.4.2.1
gene5729	Contig 28	11,457	12,408	951	*rihA* 3	purine nucleosidase	3.2.2.1

light on the metabolic pathway utilized by strain YC06, revealing that the nucleobases hypoxanthine and guanine are the products of biodegradation mediated by purine nucleosidase or PNP. This finding implies that strain YC06 is capable of metabolizing inosine and guanosine into simpler molecular constituents, such as hypoxanthine and guanine, which is similar to the previous research results [41]. Microbes facilitate the biodegradation of nucleosides into nucleobases, reducing the intestinal epithelial cells' absorption of these compounds, which consequently leads to a reduction in urate production. This mechanism is at the forefront of current research on the use of microbes to improve hyperuricemia. These results highlight its potential as an LBP candidate for modulating host purine metabolism, particularly in hyperuricemia-related pathologies.

Whole-genome analysis of *B. paranthracis* YC06 identified genes encoding hypoxanthine-guanine phosphoribosyltransferase, including *hprT*, *hpt*, and *HPRT1*, which are critical for converting hypoxanthine and guanine to inosine monophosphate (IMP) and guanosine monophosphate (GMP), respectively. However, when cultured with hypoxanthine or guanine as the sole carbon and nitrogen sources, strain YC06 exhibited no growth, indicating an inability to utilize these purines under the tested conditions. This observation is important as it highlights the complexity of metabolic pathways and the need for further investigation into the metabolic fate of purine nucleotides within YC06. It may also have implications for the use of strain YC06 in biotechnological applications, particularly if the goal is to manipulate purine metabolite levels.

Notably, the absence of amino acid decarboxylase activity, a critical safety concern in microbial therapeutics, positions this strain as a promising chassis for developing LBPs with reduced risk of biogenic amine-mediated adverse effects [42]. However, the annotated virulence factors (*cytK*, *nheA*, and *nheB*), associated with hemolytic and cytotoxic activities, raise potential concerns for in vivo applications, despite their commonality in environmental *Bacillus* spp [43, 44]. To mitigate these risks, targeted gene knockout of virulence clusters or regulatory mutations to silence toxin production could be prioritized. While the annotated β-lactamase genes (*bla1*, *bcII*) likely represent intrinsic resistance mechanisms common to *Bacillus* species, the presence of horizontally acquired antibiotic resistance genes, particularly *tet(45)* (tetracycline resistance) and *vanR* (glycopeptide resistance regulator), raises critical biosafety concerns [45, 46]. Phenotypic validation of resistance profiles using broth microdilution assays (CLSI M45 guidelines) must be conducted in subsequent research, focusing on tetracycline, β-lactams, and glycopeptides.

The comparative genomic analysis across eight *B. paranthracis* strains revealed both conserved and strain-specific genomic features that may underpin functional diversification within this species. Notably, strain YC06 harbors 842 unique genes, the highest among the analyzed strains, of which 63% encode hypothetical proteins. While these orphan genes may reflect niche-specific adaptations, a subset co-localizes with the purine degradation operon, suggesting potential auxiliary functions in nucleoside metabolism [47]. The expansive pangenome indicates substantial genomic plasticity, a trait that could enhance environmental adaptability but necessitates caution in therapeutic applications due to risks of horizontal gene transfer involving mobile elements [48].

Additionally, microbes contribute to the modulation of the gut microbiota, suppression of xanthine oxidase (XOD) activity, and enhancement of urate transporters expression [37]. These functions represent the main avenues through which microbes can ameliorate hyperuricemia and also constitute the focus of our ongoing research into the capabilities and applications of *B. paranthracis* YC06. *Bacillus* species exhibit numerous probiotic properties that position them as promising candidates for use in the human gastrointestinal tract. Their resilience in the gastrointestinal tract, as evidenced by their tolerance to acidic conditions and bile salts, along with their stability in food and pharmaceutical formulations, ensures their survival and functionality within the host. These strains are capable of producing antimicrobial peptides

and extracellular effector molecules that contribute to immune modulation through interaction with the host. Safety concerns, however, cannot be overlooked. Given the pathogenic potential of some *Bacillus* strains such as *B. cereus* and *B. anthracis*, which can produce toxins, a rigorous safety assessment is imperative for each strain to ensure that commercial and clinical applications do not pose risks to consumers. Looking ahead, further research is essential to elucidate the precise mechanisms by which *Bacillus* strains modulate the host's immune response and interact with the gut microbiota. Additional clinical trials are needed to confirm the health benefits of *Bacillus* as probiotics.

Collectively, these insights suggest that *B. paranthracis* YC06 is a promising candidate for probiotic applications, particularly for developing LBPs, which aimed at ameliorating hyperuricemia and gout by biodegrading urate precursors and thus reducing urate synthesis.

Abbreviations

ANI	Average Nucleotide Identity
PCR	Polymerase Chain Reaction
PNP	Purine-Nucleoside Phosphorylase
LB	Luria-Bertani
CEs	Cell-free Extracts
NCBI	National Center for Biotechnology Information
COG	Cluster of Orthologous Groups of proteins
GO	Gene Ontology
KEGG	Kyoto Encyclopedia of Genes and Genomes
EC	Enzyme Commission
NR	Non-redundant proteins
IMP	Inosine Monophosphate
GMP	Guanosine Monophosphate
LBP	Live Biotherapeutic Product
XOD	Xanthine Oxidase
CLSI	Clinical and Laboratory Standards Institute
CFU	Colony Forming Unit

Supplementary Information

The online version contains supplementary material available at https://doi.org/10.1186/s12866-025-04063-8.

Supplementary Material 1

Acknowledgements
We gratefully acknowledge the financial support from National Key Research and Development Program of China (Grant NO.2022YFE0118800).

Author contributions
X.C. and H.Y. conceived and designed the research. X.C. and Y.Z. performed the experiments. X.C. analyzed the data. All authors discussed the results. X.C. wrote the manuscript. Q.X. and H.Y. revised and edited the manuscript. All authors read and approved the final manuscript.

Funding
This work was financially supported by the National Key Research and Development Program of China (Grant NO. 2022YFE0118800).

Data availability
The raw genome sequence of Bacillus paranthracis YC06 has been deposited in the Sequence Read Archive (SRA) of National Center for Biotechnology Information (NCBI) under the accession number SRR29604880, and the other data will be made available on request.

Declarations

Ethics approval and consent to participate
Not applicable.

Consent for publication
Not applicable.

Statement on human and animal rights
This article does not contain any studies with human participants or animals performed by any of the authors.

Competing interests
The authors declare no competing interests.

Received: 23 August 2024 / Accepted: 20 May 2025
Published online: 28 May 2025

References

1. Dewulf JP, Marie S, Nassogne MC. Disorders of purine biosynthesis metabolism. Mol Genet Metab. 2022;136(3):190–8. https://doi.org/10.1016/j.ymgme.2021.12.016.
2. Bardin T, Richette P. Definition of hyperuricemia and gouty conditions. Curr Opin Rheumatol. 2014;26(2):186–91. https://doi.org/10.1097/BOR.0000000000000028.
3. Li L, Zhao M, Wang C, Zhang S, Yun C, Chen S, et al. Early onset of hyperuricemia is associated with increased cardiovascular disease and mortality risk. Clin Res Cardiol. 2021;110(7):1096–105. https://doi.org/10.1007/s00392-021-01849-4.
4. Kuma A, Kato A. Lifestyle-Related risk factors for the incidence and progression of chronic kidney disease in the healthy young and Middle-Aged population. Nutrients. 2022;14(18). https://doi.org/10.3390/nu14183787.
5. Yao S, Zhou Y, Xu L, Zhang Q, Bao S, Feng H, et al. Association between hyperuricemia and metabolic syndrome: A cross-sectional study in Tibetan adults on the Tibetan plateau. Front Endocrinol (Lausanne). 2022;13. https://doi.org/10.3389/fendo.2022.964872.
6. Huang J, Ma ZF, Zhang Y, Wan Z, Li Y, Zhou H, et al. Geographical distribution of hyperuricemia in Mainland China: a comprehensive systematic review and meta-analysis. Global Health Res Policy. 2020;5(1):52. https://doi.org/10.1186/s41256-020-00178-9.
7. Sun L, Ni C, Zhao J, Wang G, Chen W. Probiotics, bioactive compounds and dietary patterns for the effective management of hyperuricemia: a review. Crit Rev Food Sci Nutr. 2022;1–16. https://doi.org/10.1080/10408398.2022.2119934.
8. Stamp LK, Merriman TR, Singh JA. Expert opinion on emerging urate-lowering therapies. Expert Opin Emerg Drugs. 2018;23(3):201–9. https://doi.org/10.1080/14728214.2018.1527899.
9. Kakutani-Hatayama M, Kadoya M, Okazaki H, Kurajoh M, Shoji T, Koyama H, et al. Nonpharmacological management of gout and hyperuricemia: hints for better lifestyle. Am J Lifestyle Med. 2017;11(4):321–9. https://doi.org/10.1177/1559827615601973.
10. Strilchuk L, Fogacci F, Cicero AF. Safety and tolerability of available urate-lowering drugs: a critical review. Expert Opin Drug Saf. 2019;18(4):261–71. https://doi.org/10.1080/14740338.2019.1594771.
11. Bzowska A, Kulikowska E, Shugar D. Purine nucleoside phosphorylases: properties, functions, and clinical aspects. Pharmacol Ther. 2000;88(3):349–425. https://doi.org/10.1016/s0163-7258(00)00097-8.
12. Ferdiansyah MK, Kang HS, Kim GY, Park B, Kularathna R, Abraha HB, et al. Purine nucleosidase (PNase) activity, probiotics potential, and food applicability of a newly-isolated *Levilactobacillus brevis* LAB42. Food Sci Technol Int. 2023. https://doi.org/10.1177/10820132231219859.
13. Gil A, Gómez-León C, Rueda R. Exogenous nucleic acids and nucleotides are efficiently hydrolysed and taken up as nucleosides by intestinal explants from suckling piglets. Br J Nutr. 2007;98(2):285–91. https://doi.org/10.1017/s000711450770908x.
14. Zhao H, Chen X, Meng F, Zhou L, Pang X, Lu Z, et al. Ameliorative effect of Lacticaseibacillus rhamnosus Fmb14 from Chinese yogurt on hyperuricemia. Food Sci Hum Wellness. 2023;12(4):1379–90. https://doi.org/10.1016/j.fshw.2022.10.031.

15. Li M, Wu X, Guo Z, Gao R, Ni Z, Cui H, et al. Lactiplantibacillus plantarum enables blood urate control in mice through degradation of nucleosides in Gastrointestinal tract. Microbiome. 2023;11(1). https://doi.org/10.1186/s40168-023-01605-y.
16. Meng YP, Hu YS, Wei M, Wang KM, Wang YY, Wang SL, et al. Amelioration of hyperuricemia by Lactobacillus acidophilus F02 with uric acid-lowering ability via modulation of NLRP3 inflammasome and gut microbiota homeostasis. J Funct Foods. 2023;111. https://doi.org/10.1016/j.jff.2023.105903.
17. Lu L, Liu T, Liu X, Wang C. Screening and identification of purine degrading Lactobacillus fermentum 9–4 from Chinese fermented rice-flour noodles. Food Sci Hum Wellness. 2022;11(5):1402–8. https://doi.org/10.1016/j.fshw.2022.04.030.
18. Wang J, Chen Y, Zhong H, Chen F, Regenstein J, Hu X, et al. The gut microbiota as a target to control hyperuricemia pathogenesis: potential mechanisms and therapeutic strategies. Crit Rev Food Sci Nutr. 2022;62(14):3979–89. https://doi.org/10.1080/10408398.2021.1874287.
19. Ichida K, Matsuo H, Takada T, Nakayama A, Murakami K, Shimizu T, et al. Decreased extra-renal urate excretion is a common cause of hyperuricemia. Nat Commun. 2012;3:764. https://doi.org/10.1038/ncomms1756.
20. Yin H, Liu N, Chen J. The role of the intestine in the development of hyperuricemia. Front Immunol. 2022;13. https://doi.org/10.3389/fimmu.2022.845684.
21. Liang M, Liu J, Chen W, He Y, Kahaer M, Li R, et al. Diagnostic model for predicting hyperuricemia based on alterations of the gut Microbiome in individuals with different serum uric acid levels. Front Endocrinol (Lausanne). 2022;13:925119. https://doi.org/10.3389/fendo.2022.925119.
22. Lee N-K, Kim W-S, Paik H-D. Bacillus strains as human probiotics: characterization, safety, microbiome, and probiotic carrier. Food Sci Biotechnol. 2019;28(5):1297–305. https://doi.org/10.1007/s10068-019-00691-9.
23. Cao X, Cai J, Zhang Y, Liu C, Song M, Xu Q, et al. Biodegradation of uric acid by Bacillus paramycoides-YC02. Microorganisms. 2023;11(8). https://doi.org/10.3390/microorganisms11081989.
24. Wu Y-p, Liu D-m, Zhao S, Huang Y-y, Yu J-j. Zhou Q-y. Assessing the safety and probiotic characteristics of Bacillus coagulans 13002 based on complete genome and phenotype analysis. LWT. 2022;155. https://doi.org/10.1016/j.lwt.2021.112847.
25. Brodkorb A, Egger L, Alminger M, Alvito P, Assunção R, Ballance S, et al. INFOGEST static in vitro simulation of Gastrointestinal food digestion. Nat Protoc. 2019;14(4):991–1014. https://doi.org/10.1038/s41596-018-0119-1.
26. Diale MO, Kayitesi E, Serepa-Dlamini MH. Genome in Silico and in vitro analysis of the probiotic properties of a bacterial endophyte, Bacillus paranthracis strain MHSD3. Front Genet. 2021;12. https://doi.org/10.3389/fgene.2021.672149.
27. Wang F, Li X, Wang Q, Jin Q, Fu A, Zhang Q, et al. Based on whole genome sequencing and metabolomics analysis the safety and probiotic characteristics of Lacticaseibacillus paracasei 36 isolated from Chinese fermented vegetables. Food Bioscience. 2024;62. https://doi.org/10.1016/j.fbio.2024.105405.
28. Cordonnier C, Thévenot J, Etienne-Mesmin L, Denis S, Alric M, Livrelli V, et al. Dynamic in vitro models of the human Gastrointestinal tract as relevant tools to assess the survival of probiotic strains and their interactions with gut microbiota. Microorganisms. 2015;3(4):725–45. https://doi.org/10.3390/microorganisms3040725.
29. Luo Y, De Souza C, Ramachandran M, Wang SL, Yi HX, Ma Z, et al. Precise oral delivery systems for probiotics: A review. J Controlled Release. 2022;352:371–84. https://doi.org/10.1016/j.jconrel.2022.10.030.
30. Seo SW, Kim D, O'Brien EJ, Szubin R, Palsson BO. Decoding genome-wide GadEWX-transcriptional regulatory networks reveals multifaceted cellular responses to acid stress in Escherichia coli. Nat Commun. 2015;6(1). https://doi.org/10.1038/ncomms8970.
31. Senouci-Rezkallah K, Jobin MP, Schmitt P. Adaptive responses of *Bacillus cereus* ATCC14579 cells upon exposure to acid conditions involve ATPase activity to maintain their internal pH. MicrobiologyOpen. 2015;4(2):313–22;. https://doi.org/10.1002/mbo3.239
32. Chun BH, Kim KH, Jeong SE, Jeon CO. Genomic and metabolic features of the *Bacillus amyloliquefaciens* group—*B. amyloliquefaciens*, *B. velezensis*, and *B. siamensis*—revealed by pan-genome analysis. Food Microbiol. 2019;77:146–57;. https://doi.org/10.1016/j.fm.2018.09.001
33. Macierzanka A, Torcello-Gómez A, Jungnickel C, Maldonado-Valderrama J. Bile salts in digestion and transport of lipids. Adv Colloid Interface Sci. 2019;274. https://doi.org/10.1016/j.cis.2019.102045.
34. Lambert JM, Bongers RS, de Vos WM, Kleerebezem M. Functional analysis of four bile salt hydrolase and penicillin acylase family members in *Lactobacillus plantarum* WCFS1. Appl Environ Microbiol. 2008;74(15):4719–26. https://doi.org/10.1128/aem.00137-08.
35. Rossi GAM, Silva HO, Aguilar CEG, Rochetti AL, Pascoe B, Méric G, et al. Comparative genomic survey of *Bacillus cereus sensu stricto* isolates from the dairy production chain in Brazil. FEMS Microbiol Lett. 2018;365(3). https://doi.org/10.1093/femsle/fnx283.
36. Wójcik W, Lukasiewicz M, Puppel K. Biogenic amines: formation, action and toxicity - a review. J Sci Food Agric. 2021;101(7):2634–40. https://doi.org/10.1002/jsfa.10928.
37. Zhao H, Lu Z, Lu Y. The potential of probiotics in the amelioration of hyperuricemia. Food Funct. 2022;13(5):2394–414. https://doi.org/10.1039/d1fo03206b.
38. Liu Y, Du J, Lai Q, Zeng R, Ye D, Xu J, et al. Proposal of nine novel species of the Bacillus cereus group. Int J Syst Evol Microbiol. 2017;67(8):2499–508. https://doi.org/10.1099/ijsem.0.001821.
39. Lozupone CA, Stombaugh JI, Gordon JI, Jansson JK, Knight R. Diversity, stability and resilience of the human gut microbiota. Nature. 2012;489(7415):220–30. https://doi.org/10.1038/nature11550.
40. Du X, Jiang Y, Sun Y, Cao X, Zhang Y, Xu Q, et al. Biodegradation of inosine and Guanosine by Bacillus paranthracis YD01. Int J Mol Sci. 2023;24(19). https://doi.org/10.3390/ijms241914462.
41. Kuo YW, Hsieh SH, Chen JF, Liu CR, Chen CW, Huang YF, et al. Lactobacillus reuteri TSR332 and Lactobacillus fermentum TSF331 stabilize serum uric acid levels and prevent hyperuricemia in rats. PeerJ. 2021;9:e11209. https://doi.org/10.7717/peerj.11209.
42. Doeun D, Davaatseren M, Chung MS. Biogenic amines in foods. Food Sci Biotechnol. 2017;26(6):1463–74. https://doi.org/10.1007/s10068-017-0239-3.
43. Li P, Tian WN, Jiang Z, Liang ZH, Wu XY, Du B. Genomic characterization and probiotic potency of *Bacillus* sp DU-106, a highly effective producer of L-Lactic acid isolated from fermented yogurt. Front Microbiol. 2018;9. https://doi.org/10.3389/fmicb.2018.02216.
44. Johnson SL, Daligault HE, Davenport KW, Jaissle J, Frey KG, Ladner JT, et al. Complete genome sequences for 35 biothreat Assay-Relevant Bacillus species. Genome Announcements. 2015;3(2). https://doi.org/10.1128/genomeA.00151-15.
45. Ma JL, Liu J, Zhang Y, Wang D, Liu RX, Liu GJ, et al. Bacitracin resistance and enhanced virulence of *Streptococcus suis* via a novel efflux pump. BMC Vet Res. 2019;15(1). https://doi.org/10.1186/s12917-019-2115-2.
46. Khatri I, Sharma G, Subramanian S. Composite genome sequence of *Bacillus clausii*, a probiotic commercially available as Enterogermina®, and insights into its probiotic properties. BMC Microbiol. 2019;19(1). https://doi.org/10.1186/s12866-019-1680-7.
47. Iwadate Y, Kato J. Identification of a Formate-Dependent uric acid degradation pathway in *Escherichia coli*. J Bacteriol. 2019;201(11). https://doi.org/10.1128/jb.00573-18.
48. Tokuda M, Shintani M. Microbial evolution through horizontal gene transfer by mobile genetic elements. Microb Biotechnol. 2024;17(1). https://doi.org/10.1111/1751-7915.14408.

Publisher's note